ISSN 1007-9327 (print)
ISSN 2219-2840 (online)

World Journal of *Gastroenterology*

World J Gastroenterol 2019 October 28; 25(40): 6041-6171

Published by Baishideng Publishing Group Inc

World Journal of Gastroenterology

Contents

Weekly Volume 25 Number 40 October 28, 2019

REVIEW

MINIREVIEWS

ORIGINAL ARTICLE

Basic Study

Retrospective Study

Clinical Trials Study

Observational Study

Randomized Clinical Trial

Contents

World Journal of Gastroenterology

Volume 25 Number 40 October 28, 2019

ABOUT COVER

Editorial board member of *World Journal of Gastroenterology*, Mark D Gorrell, PhD, Professor, Liver Enzymes in Metabolism and Inflammation Program, Centenary Institute and University of Sydney, Sydney 2006, NSW, Australia

AIMS AND SCOPE

The primary aim of *World Journal of Gastroenterology* (*WJG*, *World J Gastroenterol*) is to provide scholars and readers from various fields of gastroenterology and hepatology with a platform to publish high-quality basic and clinical research articles and communicate their research findings online.

WJG mainly publishes articles reporting research results and findings obtained in the field of gastroenterology and hepatology and covering a wide range of topics including gastroenterology, hepatology, gastrointestinal endoscopy, gastrointestinal surgery, gastrointestinal oncology, and pediatric gastroenterology.

INDEXING/ABSTRACTING

The *WJG* is now indexed in Current Contents®/Clinical Medicine, Science Citation Index Expanded (also known as SciSearch®), Journal Citation Reports®, Index Medicus, MEDLINE, PubMed, PubMed Central, and Scopus. The 2019 edition of Journal Citation Report® cites the 2018 impact factor for *WJG* as 3.411 (5-year impact factor: 3.579), ranking *WJG* as 35th among 84 journals in gastroenterology and hepatology (quartile in category Q2). CiteScore (2018): 3.43.

RESPONSIBLE EDITORS FOR THIS ISSUE

Responsible Electronic Editor: *Yan-Liang Zhang*

Proofing Production Department Director: *Xiang Li*

NAME OF JOURNAL
World Journal of Gastroenterology

ISSN
ISSN 1007-9327 (print) ISSN 2219-2840 (online)

LAUNCH DATE
October 1, 1995

FREQUENCY
Weekly

EDITORS-IN-CHIEF
Subrata Ghosh, Andrzej S Tarnawski

EDITORIAL BOARD MEMBERS
http://www.wjgnet.com/1007-9327/editorialboard.htm

EDITORIAL OFFICE
Ze-Mao Gong, Director

PUBLICATION DATE
October 28, 2019

INSTRUCTIONS TO AUTHORS
https://www.wjgnet.com/bpg/gerinfo/204

GUIDELINES FOR ETHICS DOCUMENTS
https://www.wjgnet.com/bpg/GerInfo/287

GUIDELINES FOR NON-NATIVE SPEAKERS OF ENGLISH
https://www.wjgnet.com/bpg/gerinfo/240

PUBLICATION MISCONDUCT
https://www.wjgnet.com/bpg/gerinfo/208

ARTICLE PROCESSING CHARGE
https://www.wjgnet.com/bpg/gerinfo/242

STEPS FOR SUBMITTING MANUSCRIPTS
https://www.wjgnet.com/bpg/GerInfo/239

ONLINE SUBMISSION
https://www.f6publishing.com

World Journal of Gastroenterology

Submit a Manuscript: https://www.f6publishing.com

World J Gastroenterol 2019 October 28; 25(40): 6116-6128

DOI: 10.3748/wjg.v25.i40.6116

ISSN 1007-9327 (print) ISSN 2219-2840 (online)

ORIGINAL ARTICLE

Retrospective Study

Apparent diffusion coefficient-based histogram analysis differentiates histological subtypes of periampullary adenocarcinoma

Jing-Yu Lu, Hao Yu, Xian-Lun Zou, Zhen Li, Xue-Mei Hu, Ya-Qi Shen, Dao-Yu Hu

ORCID number: Jing-Yu Lu (0000-0001-7364-9693); Hao Yu (0000-0002-4495-897X); Xian-Lun Zou (0000-0002-1836-6102); Zhen Li (0000-0002-9289-6785); Xue-Mei Hu (0000-0001-9009-0983); Ya-Qi Shen (0000-0003-0589-8975); Dao-Yu Hu (0000-0001-9281-8552).

Author contributions: All authors contributed to the design of the study; Lu JY and Shen YQ wrote the manuscript; Yu H and Hu XM contributed to the measurement; Lu JY and Zou XL contributed to data acquisition and prepared the tables and figures; Li Z, Shen YQ, and Hu DY revised the manuscript; all authors reviewed the manuscript and approved the final vision to be submitted.

Supported by the National Natural Science Foundation of China, No. 81701657, No. 81571642, No. 81801695, and No. 81771801; the Fundamental Research Funds for the Central Universities, No. 2017KFYXJJ126.

Institutional review board statement: This study was approved by the Ethics Committee of Tongji Hospital, Tongji Medical College, Huazhong University of Science and Technology.

Informed consent statement: All patients agreed to MR examination and treatment with written consent. Due to the retrospective nature of the present study, the additional informed consent was waived.

Jing-Yu Lu, Hao Yu, Xian-Lun Zou, Zhen Li, Xue-Mei Hu, Ya-Qi Shen, Dao-Yu Hu, Department of Radiology, Tongji Hospital, Tongji Medical College, Huazhong University of Science and Technology, Wuhan 430030, Hubei Province, China

Jing-Yu Lu, Department of Radiology, the First Affiliated Hospital of Soochow University, Suzhou 215006, Jiangsu Province, China

Corresponding author: Ya-Qi Shen, MD, PhD, Doctor, Department of Radiology, Tongji Hospital, Tongji Medical College, Huazhong University of Science and Technology,1095 Jiefang Avenue, Wuhan 430030, Hubei Province, China. yqshen@hust.edu.cn
Telephone: +86-27-83662640
Fax: +86-27-83662640

Abstract

BACKGROUND

For periampullary adenocarcinoma, the histological subtype is a better prognostic predictor than the site of tumor origin. Intestinal-type periampullary adenocarcinoma (IPAC) is reported to have a better prognosis than the pancreatobiliary-type periampullary adenocarcinoma (PPAC). However, the classification of histological subtypes is difficult to determine before surgery. Apparent diffusion coefficient (ADC) histogram analysis is a noninvasive, non-enhanced method with high reproducibility that could help differentiate the two subtypes.

AIM

To investigate whether volumetric ADC histogram analysis is helpful for distinguishing IPAC from PPAC.

METHODS

Between January 2015 and October 2018, 476 consecutive patients who were suspected of having a periampullary tumor and underwent magnetic resonance imaging (MRI) were reviewed in this retrospective study. Only patients who underwent MRI at 3.0 T with different diffusion-weighted images (*b*-values = 800 and 1000 s/mm^2) and who were confirmed with a periampullary adenocarcinoma were further analyzed. Then, the mean, 5th, 10th, 25th, 50th, 75th, 90th, and 95th percentiles of ADC values and ADC_{min}, ADC_{max}, kurtosis, skewness, and entropy were obtained from the volumetric histogram analysis. Comparisons were made by an independent Student's *t*-test or Mann-Whitney *U*

Conflict-of-interest statement: All authors declare no conflicts of interest related to this article.

Data sharing statement: No additional data are available.

Manuscript source: Unsolicited manuscript

Received: July 23, 2019
Peer-review started: July 23, 2019
First decision: August 27, 2019
Revised: September 17, 2019
Accepted: September 27, 2019
Article in press: September 28, 2019
Published online: October 28, 2019

P-Reviewer: Tabibian JH
S-Editor: Tang JZ
L-Editor: Wang TQ
E-Editor: Zhang YL

test. Multiple-class receiver operating characteristic curve analysis was performed to determine and compare the diagnostic value of each significant parameter.

RESULTS

In total, 40 patients with histopathologically confirmed IPAC (n = 17) or PPAC (n = 23) were enrolled. The mean, 5th, 25th, 50th, 75th, 90th, and 95th percentiles and ADC_{max} derived from ADC_{1000} were significantly lower in the PPAC group than in the IPAC group ($P < 0.05$). However, values derived from ADC_{800} showed no significant difference between the two groups. The 75th percentile of ADC_{1000} values achieved the highest area under the curve (AUC) for differentiating IPAC from PPAC (AUC = 0.781; sensitivity, 91%; specificity, 59%; cut-off value, 1.50 × 10^{-3} mm^2/s).

CONCLUSION

Volumetric ADC histogram analysis at a b-value of 1000 s/mm^2 might be helpful for differentiating the histological subtypes of periampullary adenocarcinoma before surgery.

Key words: Periampullary adenocarcinoma; Apparent diffusion coefficient; Histogram analysis; Histopathology; Differential diagnosis

Core tip: Two subtypes of periampullary adenocarcinoma were investigated in the present study: one is intestinal-type periampullary adenocarcinoma (IPAC), and the other is pancreatobiliary-type periampullary adenocarcinoma (PPAC). The aim of the present study was to distinguish these two subtypes by volumetric apparent diffusion coefficient (ADC) histogram analysis. Forty pathologically confirmed patients were enrolled. The mean, maximum, and various percentiles of ADC values derived from b_{1000} were lower in the PPAC group than in the IPAC group with statistical significance. The 75th percentile of ADC values achieved the highest area under the curve.

Citation: Lu JY, Yu H, Zou XL, Li Z, Hu XM, Shen YQ, Hu DY. Apparent diffusion coefficient-based histogram analysis differentiates histological subtypes of periampullary adenocarcinoma. *World J Gastroenterol* 2019; 25(40): 6116-6128
URL: https://www.wjgnet.com/1007-9327/full/v25/i40/6116.htm
DOI: https://dx.doi.org/10.3748/wjg.v25.i40.6116

INTRODUCTION

Periampullary adenocarcinomas comprise adenocarcinomas of the ampulla, distal common bile duct, pancreas, and duodenum, arising within 2 cm of the major duodenal papilla[1]. However, due to the complexity of the periampullary region, misclassification of the original tumor site occurs in clinical practice[2]. Although resectable periampullary adenocarcinomas from different tumor origins are treated similarly by curative pancreatoduodenectomy (PD)[3], the prognosis varies considerably with a 5-year survival rate ranging from 34% to 66%[4]. Although improved outcome for patients with pancreatic adenocarcinoma receiving adjuvant chemotherapy has been demonstrated, the role of adjuvant therapy in nonpancreatic periampullary adenocarcinomas is less clear, which indicates the histological heterogeneity of the periampullary malignancy[5,6].

To better predict the prognosis of periampullary adenocarcinomas and to guide pre- and postoperative treatment, a classification based on histopathological subtype instead of anatomical origin was developed. Intestinal-type periampullary adenocarcinoma (IPAC) was reported to have a better prognosis than pancreatobiliary-type periampullary adenocarcinoma (PPAC)[3,4,7-9]. Patients with IPAC had a median overall survival of 71.7 mo, while patients with PPAC had a median overall survival of only 33.3 mo[7]. These two subtypes show contrasting response to different chemotherapeutic regimens. The PPAC tends to respond better to gemcitabine-based therapies, while the IPAC responds better to flu-oropyrimidine[10].

Thus, the histological subtypes should be taken into consideration when deriving therapeutic strategies[5,11].

At present, the classification of histological subtypes mainly relies on standardized dissected PD specimens[2]. Unfortunately, patients with peripheral vessel involvement or metastatic malignancy rarely benefit from PD[12-14]. It is also difficult for contrast-enhanced computed tomography (CT) or multiparameter magnetic resonance imaging (MRI) to classify the histological subtypes before surgery.

A qualitative study found that the comprehensive evaluation of multiple CT features of the periampullary area could differentiate the histological subtypes, but required optimal duodenal distention and was highly dependent on the expertise of the radiologists[15]. An oval filling defect at the end of the bile duct on magnetic resonance cholangiopancreatography images tended to suggest IPAC but controversy still existed[16,17].

Diffusion-weighted imaging (DWI) is a functional MRI method. It calculates the apparent diffusion coefficient (ADC) to reflect random motion of water molecules, which could add information pertinent to tissue structure. Bi *et al*[16] found a combination of a progressive enhancement pattern and low minimum ADC value (b_{800}) suggestive of PPAC, but the diagnostic performance of ADC_{min} alone was not high enough. In addition, the use of gadolinium-based contrast agents is limited in patients with impaired renal function[18,19]. Thus, a non-invasive and non-contrast-enhanced method before surgery is needed.

Volumetric ADC histogram parameters reflect the distribution and variation of all voxels within the entire lesion, which reduce the subjectivity of region of interest (ROI) placement and improve repeatability in the quantitative ADC analysis[20,21]. Previous studies have applied volumetric ADC histogram analysis to differentiate histopathological subtypes of renal cell carcinomas, breast cancers, and ovarian cancers[20,22-24]. No ADC histogram study thus far has focused on periampullary adenocarcinomas.

Therefore, the aim of this study was to investigate the diagnostic value of volumetric ADC histogram analysis in the differentiation of IPAC and PPAC.

MATERIALS AND METHODS

Study cohort

This retrospective study was approved by the local institutional review board, and the requirement for informed consent was waived. After searching the radiological database from January 2015 to October 2018, 476 consecutive patients who were suspected of having periampullary tumor and underwent preoperative MRI were identified. The inclusion criteria for this study were as follows: (1) MRI acquired at 3.0 T; and (2) Diffusion weighted imaging administered at *b*-values of 800 and 1000 s/mm^2. The exclusion criteria were as follows: (1) Patients discharged without receiving radical surgery at our institution; (2) Patients histopathologically confirmed with lesions other than IPAC or PPAC; (3) Patients who received invasive treatment before MRI; and (4) Poor image quality for analysis. The flowchart of the study population is shown in Figure 1.

Image acquisition

All patients were required to fast for 6-8 h before MRI acquisition. All scans were performed on a 3 T MRI scanner (GE Healthcare 750 discovery, United States) using a 32-channel torso array coil. Before DWI, the routine protocol included the following sequences: (1) Coronal SSFSE sequence [repetition time/echo time (TR/TE), 1363.0 ms/80 ms; matrix, 256 × 256; FOV, 36-44 cm; slice thickness, 5 mm]; (2) Transverse T1-weighted (LAVA-FLEX) image (TR/TE, 3.7 ms/2.0 ms; matrix, 256 × 256; FOV, 36-44 cm; slice thickness, 4 mm; intersection gap, 0 mm); and (3) Axial respiratory-triggered T2-weighted image (TR/TE, 7059 ms/63 ms; matrix, 320 × 320; FOV, 36–44 cm; slice thickness, 4 mm; intersection gap, 1 mm). For DWI, respiratory-triggered single-shot echo-planar sequences in the axial plane were performed [matrix, 160 × 192; FOV, 36-44 cm; slice thickness, 4 mm; intersection gap, 1 mm; bandwidth, 250 kHz/pixel; acquisition time, 4-5 min; flip angle, 90°; the number of excitations (NEX), 6], and images at *b*-values of 0, 800, and 1000 s/mm^2 were acquired in three orthogonal diffusion directions.

Image analysis

All raw data from DWI were transferred from the picture archiving and communication system (PACS) to a PC and processed with the open source software Fire voxel (https://files.nyu.edu/hr18/public/projects.html). Two independent

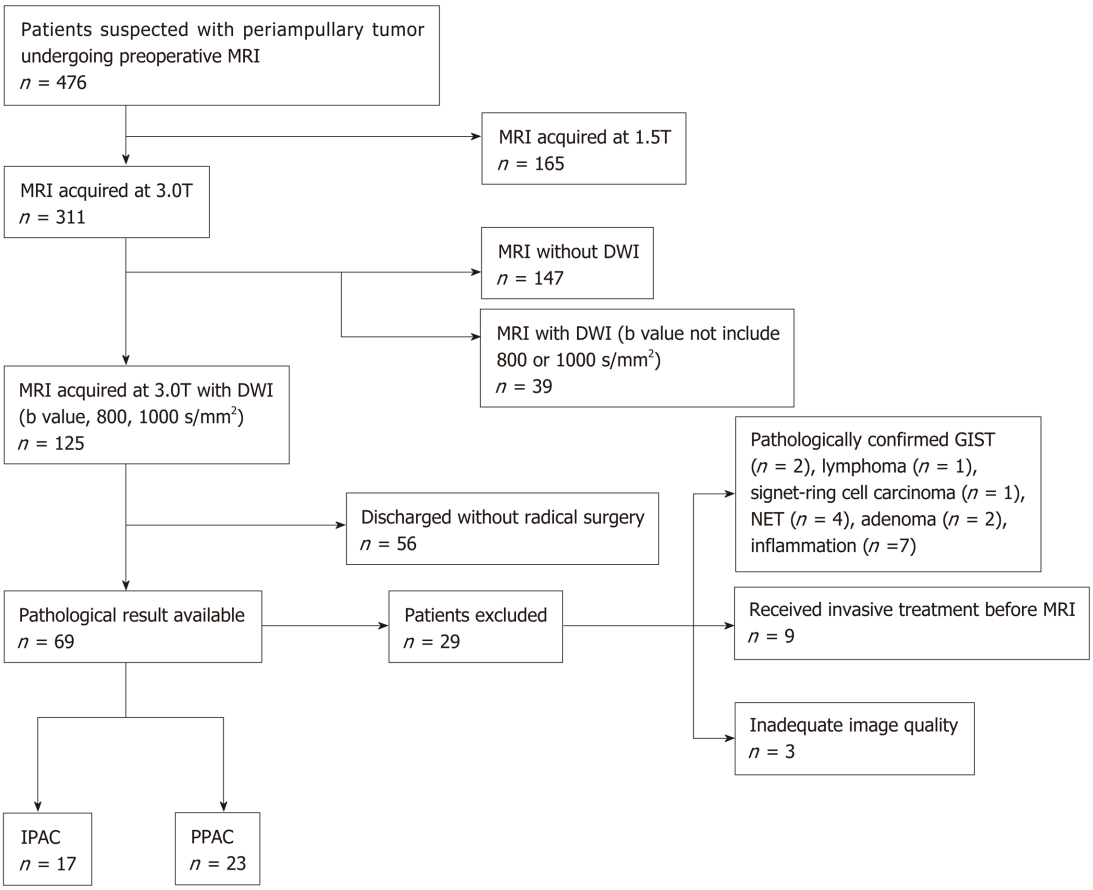

Figure 1 Flowchart of the study cohort. MRI: Magnetic resonance imaging; DWI: Diffusion-weighted imaging; IPAC: Intestinal-typeperiampullary adenocarcinoma; PPAC: Pancreatobiliary-type periampullary adenocarcinoma; GIST: Gastric gastrointestinal stromal tumor; NET: Neuroendocrine tumor.

radiologists (with 4 and 15 years of experience in abdominal MRI, respectively) blinded to the clinical information and histopathologic results independently reviewed all the MR images. They manually drew the ROI covering the lesion at each section with reference to the axial T2-weighted images. Care was taken to avoid regions of artefacts. The ROI of each layer was merged automatically into a volumetric ROI containing voxel information of the whole tumor. A volumetric ADC map was then constructed with a monoexponential fitting model: $S = S_0 \exp(-b \times ADC)$, where S represents diffusion-induced signal attenuation, S_0 represents the signal intensity in the absence of diffusion sensitization, and b is known as the *b*-value, which determines the degree of diffusion weighting in the signal. The histogram parameters, including the mean, 5th, 10th, 25th, 50th, 75th, 90th, and 95th percentile ADC values, ADC_{min}, and ADC_{max} as well as skewness, kurtosis, and entropy, were calculated.

Histopathologic analysis

Tissue sections were stained after surgery with haematoxylin and eosin, and the microscopic slides and histopathologic reports of all patients were reviewed. Tumor size, tumor differentiation grade, perineural invasion, vessel involvement, regional nodal involvement, and histological subtype were investigated. The histological subtype was classified by morphological assessment according to the criteria first suggested by Kimura *et al*[25] and the WHO classification[26]. In brief, IPAC is characterized by well-formed tubular to elongated glands and solid nests similar to colon cancer. The tumor cells are tall and often pseudostratified columnar epitheliums with oval-or cigar-shaped nuclei. PPAC has simple or branching glands and small solid nests of cells surrounded by a desmoplastic stroma. The tumor cells are cuboidal to low columnar epithelium arranged in a single layer[3,9,27,28].

Statistical analysis

All statistical analyses were conducted with MedCalc (MedCalc Software, Mariakerke, Belgium) and IBM SPSS 23.0 (Chicago, IL, United States). The differences in the clinical and histopathological characteristics of the patients were tested by

Mann-Whitney U test or the chi-squared test. Interobserver consistency of the measurements between the two radiologists was assessed by calculating the interclass correlation coefficient (ICC). ICC > 0.80 was considered to indicate excellent agreement. Parameters with ICC < 0.8 were excluded from further statistical analyses. Then, the Shapiro-Wilk test was used to determine whether the variables were normally distributed. The Student's *t*-test or the Mann-Whitney U test was used to compare the differences between two histological groups. $P < 0.05$ was deemed to be statistically significant. Receiver operating characteristic (ROC) analyses were further performed to determine the potential diagnostic performance for differentiating the histological subtypes. The optimal threshold was chosen according to the Youden index.

RESULTS

Study population

A total of 40 histopathologically confirmed subjects were included in this retrospective study. According to the pathologic results, 17 patients had IPAC (12 males and 5 females; age range, 44–69 years), while 23 patients had PPAC (14 males and 9 females; age range, 42–69 years). The clinical characteristics and histopathological findings of the included patients are presented in Table 1. There was no significant difference in age ($P = 0.929$), sex ratio ($P = 0.524$), tumor size ($P = 0.273$), degree of tumor differentiation ($P = 0.288$), lymph node metastasis ($P = 0.893$), or vessel involvement ($P = 0.904$) between the two histological groups. Carbohydrate antigen 19-9 (CA19-9) was elevated (> 34 U/mL) in 53% (9/17) of IPACs and 65% (15/23) of PPACs ($P = 0.433$). The incidence of perineural invasion in the PPAC group was significantly higher than that in the IPAC group ($P = 0.016$).

Interobserver agreement

For all the histogram parameters except for kurtosis and skewness (ICCs < 0.8), the interobserver agreement between two readers was excellent (ICCs ranging from 0.948 to 0.996), as shown in Table 2. Thus, kurtosis and skewness were not used for the statistical analysis between the two subtypes. The mean, 5th, 10th, 25th, 50th, 75th, 90th, and 95th percentiles of ADC values, ADC_{min}, $ADC_{max,}$ and entropy were further evaluated.

Histogram parameter comparison

The ADC histogram results are summarized in Table 3 and Figure 2. The mean, 5th, 10th, 25th, 50th, 75th, 90th, and 95th percentile ADC values and ADC_{min} and ADC_{max} of IPACs were higher than those of PPACs (*b*-values = 800 and 1000 s/mm^2). At a *b*-value of 1000s/mm^2, the mean, 10th, 25th, 50th, 75th, 90th, and 95th percentile ADC values and ADC_{max} showed significant differences between the IPAC and PPAC groups ($P = 0.009$, 0.040, 0.030, 0.011, 0.004, 0.004, 0.010, and 0.008, respectively). None of the ADC_{800} histogram parameters showed significant differences between the two groups ($P > 0.05$).

Diagnostic performance of the histogram parameters

The results of the ROC analysis are shown in Table 4 and Figure 3. The 75th percentile ADC_{1000} value achieved the highest area under the curve (AUC) for differentiating IPAC from PPAC (AUC = 0.781; 95%CI: 0.623-0.896; sensitivity, 91%; specificity, 59%; cut-off value, 1.50×10^{-3} mm^2/s).

Lesions from the two subtypes of periampullary adenocarcinoma and the corresponding volumetric histogram are shown in Figures 4-6.

DISCUSSION

Accurate preoperative differentiation between IPAC and PPAC is essential for predicting the prognosis and choosing chemotherapy regimens for patients with advanced periampullary adenocarcinoma. The primary results in the present study showed that these two subtypes could be differentiated by utilizing volumetric ADC histogram analysis.

IPAC and PPAC arise from two different epithelia and may be associated with the expression of different oncogenes, immunohistochemical markers, and interactions with the extracellular matrix[2,29]. Biomarkers for intermediate filaments (CK7 and CK20) and mucins (MUC2) and the intestinal transcription factor (CDX2) were reported to be of value in separating the two histological types[8,28]. At the genetic

Table 1 Characteristics of patients enrolled in the two histological groups

	IPAC	PPAC	*P* value
Total (*n*)	17	23	
Age, yr (mean ± SD)	58.1±8.4	57.8±7.8	0.929
Male/female, *n*	12/5	14/9	0.524
CA19-9 positive (*n*)	9	15	0.433
Size, mm (mean ± SD)	15.5±5.1	17.4±5.7	0.273
Tumor differentiation	4/10/3	2/13/8	0.288
Well/moderate/poor (*n*)			
Nodal involvement (*n*)	4	5	0.893
Perineural invasion (*n*)	1	9	0.016
Vessel involvement (*n*)	2	3	0.904

CA19-9 > 34 U/mL was defined as positive. IPAC: Intestinal-type periampullary adenocarcinoma; PPAC: Pancreatobiliary-type periampullary adenocarcinoma; SD: Standard deviation; *n*: Number; CA19-9: Carbohydrate antigen 19-9.

level, a gain of 13q and 3q, and a deletion of 5q were found specifically in the intestinal-type group, and the mRNAs and miRNAs expressed between the two subtypes were different[30-32]. However, all these methods can be applied only after surgery.

In the present study, the ADC values of the IPACs were higher than those of the PPACs, which corresponded to the ADC quantitative analysis by Bi *et al*[16]. In their study, the mean ADC could not help differentiate these two histological groups, but ADC_{min} achieved a significant difference (P = 0.047; sensitivity, 85.2%; specificity, 50%; AUC = 0.672). However, the present study showed that the differences in all the ADC_{800} histogram parameters including ADC_{min} were not significant. The *b*-value of 1000 s/mm^2 seemed to better distinguish between IPAC and PPAC, as the mean, 25th, 50th, 75th, 90th, and 95th percentile ADC values and ADC_{max} showed significant differences. The difference in ADC_{min} derived from both *b*-values of 800 s/mm^2 and 1000 s/mm^2 was not significant. This finding may be explained by the different methods of ADC_{min} acquisition and different patient cohorts. In our study, ADC_{min} reflects the minimum ADC value of the whole lesion, while in the Bi's study, ADC_{min} was calculated from the largest cross-section lesion.

ADC_{1000} could better predict the histological subtypes of periampullary adenocarcinoma compared with ADC_{800} in the present study. ADC values reflect the Brownian movement of random water and are correlated with the microenvironment of tumor structures, such as tumor cellularity, the integrity of cell membranes, and the extracellular matrix[33-35]. At *b*-values ranging from 200 to 1000 s/mm^2, the degree of diffusion related signal attenuation is nearly straight, in line with Gaussian diffusion, but at a higher *b*-value range (>1000 s/mm^2), diffusion is non-Gaussian and the ADC value decreases when high *b*-values are used[36].To choose the optimal *b*-value, the location of lesions, tissue composition, and pathological features should be taken into consideration[37]. In a radiomic analysis of cervical cancer regarding histopathological grade, the overall misclassification error of ADC_{1000} features was lower compared with that of ADC_{800}[38]. In an ADC study of rectal cancer, the combination of 0 and 1000 s/mm^2 was optimal considering both reliability and diagnostic performance[39].

Volumetric ADC histogram is a possible method to identify these two histological types noninvasively before surgery. In previous studies, the ADC histogram parameters were found to be helpful in discriminating different subtypes of mucinous breast carcinoma and two epithelial types of ovarian cancer[23,40].Interestingly, the results from previous studies showed significantly lower ADC values in the more aggressive subtype than in the relatively indolent subtype, as in our research. In the present study, the 75th percentile ADC_{1000} achieved the highest AUC, and the sensitivity reached 91%. This result suggests that ADC values might have the ability to reflect the differences in microstructure between the two subtypes.

In the current study, the interobserver consistency of skewness and kurtosis was low (ICCs < 0.8). The small size of the periampullary lesions in our study could be a possible reason for this result, as the number of calculated voxels was not large enough to obtain reliable skewness and kurtosis values. The intrinsic instability of skewness and kurtosis could be another reason, as a previous repeatability study of ADC histogram metrics showed the low repeatability of skewness and kurtosis in analysing uterine lesions[41].

Table 2 Interobserver agreement for volumetric histogram parameters

	b = 800 s/mm²		*b* = 1000 s/mm²	
ADC parameter	ICC	95%CI	ICC	95%CI
Mean	0.992	0.984-0.996	0.994	0.989-0.997
Entropy	0.959	0.922-0.978	0.952	0.910-0.975
Skewness	0.742	0.153-0.864	0.781	0.585-0.884
Kurtosis	0.399	-0.136-0.682	0.486	0.029-0.728
5th	0.954	0.912-0.976	0.978	0.959-0.989
10th	0.974	0.950-0.986	0.975	0.952-0.987
25th	0.988	0.976-0.993	0.991	0.983-0.995
50th	0.989	0.978-0.994	0.996	0.992-0.998
75th	0.984	0.969-0.991	0.992	0.985-0.996
90th	0.973	0.948-0.986	0.981	0.965-0.990
95th	0.975	0.950-0.987	0.977	0.966-0.988
ADC_{min}	0.981	0.965-0.990	0.984	0.970-0.992
ADC_{max}	0.951	0.908-0.974	0.948	0.901-0.972

ICC: Interclass correlation coefficient; CI: Confidence interval; ADC: Apparent diffusion coefficient.

No significant difference in the entropy between IPAC and PPAC was found in the current study. Entropy describes the homogeneity and irregularity of the intra-lesion voxel distribution[42]. The similar entropy in the two groups suggested that the two subtypes of periampullary adenocarcinoma have high heterogeneity. In a previous histogram analysis, the entropy of ADC values showed the highest diagnostic performance in differentiation between adrenal pheochromocytoma and adenoma[43]. In liver malignancies, the entropy of cholangiocarcinoma was reported to be significantly higher than that of hepatocellular carcinoma[44]. Entropy seemed to have potential value in the differentiation of different tumor types, but limited value in the classification of different histological tumor subtypes.

Several limitations in the present study should not be ignored. First, given the retrospective nature of the present study, the subjects with an advanced tumor stage or senior patients could not tolerate radical PD and were thus excluded. Second, as strict inclusion criteria were used in the present study, the number of patients enrolled was comparatively small and they only represent a small proportion of the patients with periampullary adenocarcinoma. The conclusion from the present study needs to be confirmed in the further studies. Finally, high *b*-values (>1000s/mm²) were not used for the ADC histogram analysis in this study. Further study is warranted to strengthen the results of the ADC evaluation.

In conclusion, our study showed that volumetric ADC histogram analysis at a *b*-value of 1000 s/mm² could help differentiate IPAC and PPAC noninvasively before surgery. The 75th percentile ADC_{1000} value achieved the best diagnostic performance.

Table 3 Results of apparent diffusion coefficient histogram analysis between intestinal-type and pancreatobiliary-type periampullary adenocarcinoma

	b = 800 s/mm²			b = 1000 s/mm²		
	IPAC	PPAC	*P*	IPAC	PPAC	*P*
Mean	1.38±0.33	1.24±0.24	0.146	1.33±0.25	1.11±0.25	0.009
5th	1.01 ± 0.23	0.93 ± 0.25	0.312	0.99 ± 0.22	0.85 ± 0.27	0.094
10th	1.07 ± 0.24	0.99 ± 0.24	0.259	1.06 ± 0.23	0.89 ± 0.26	0.040
25th	1.22 ± 0.31	1.09 ± 0.24	0.146	1.16 ± 0.24	0.99 ± 0.25	0.030
50th	1.37 ± 0.33	1.23 ± 0.24	0.123	1.31 ± 0.25	1.09 ± 0.25	0.011
75th	1.51 ± 0.37	1.36 ± 0.25	0.159	1.47 ± 0.28	1.21 ± 0.25	0.004
90th	1.66 ± 0.40	1.49 ± 0.28	0.136	1.61 ± 0.32	1.32 ± 0.26	0.004
95th	1.76 ± 0.42	1.56 ± 0.30	0.136	1.68 ± 0.33	1.40 ± 0.28	0.010
ADC_{min}	0.87±0.32	0.82±0.30	0.583	0.89±0.24	0.79±0.27	0.227
ADC_{max}	1.93±0.51	1.73±0.37	0.178	1.84±0.32	1.54±0.36	0.008
Entropy	3.56±0.55	3.55±0.56	0.926	3.46±0.56	3.40±0.60	0.748

Apparent diffusion coefficient values are expressed as $\times 10^{-3}$ mm²/s. IPAC: Intestinal-type periampullary adenocarcinoma; PPAC: Pancreatobiliary-type periampullary adenocarcinoma; ADC: Apparent diffusion coefficient.

Table 4 Diagnostic performance of the volumetric histogram parameters at b_{1000}

ADC parameter	AUC (95%CI)	Cut-off (10^{-3} mm²/s)	Sensitivity (%)	Specificity (%)
Mean	0.762(0.601-0.882)	1.40	91	52
5th	0.703 (0.538-0.837)	1.09	78	58
10th	0.723 (0.558-0.825)	0.90	57	82
25th	0.742 (0.579-0.867)	1.34	83	59
50th	0.781 (0.623 0.896)	1.50	91	59
75th	0.774 (0.613-0.892)	1.44	78	69
90th	0.750 (0.581-0.877)	1.52	82	67
ADC_{max}	0.747(0.585-0.871)	1.63	70	82

ADC: Apparent diffusion coefficient; AUC: Area under the curve; CI: Confidence interval.

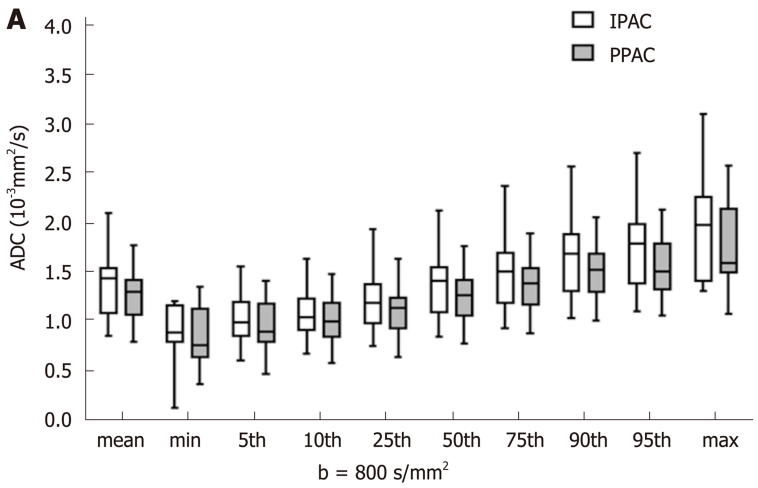

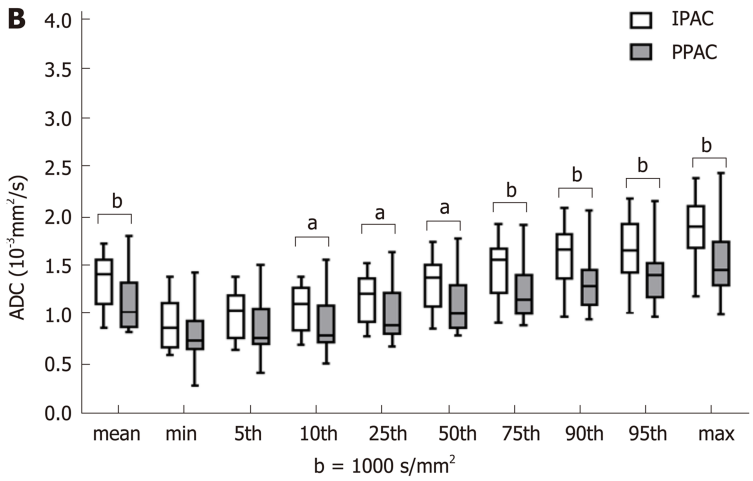

Figure 2 Box plots of the histogram parameters. [a]*P* < 0.05, [b]*P* < 0.01. IPAC: Intestinal-type periampullary adenocarcinoma; PPAC: Pancreatobiliary-type periampullary adenocarcinoma; ADC: Apparent diffusion coefficient.

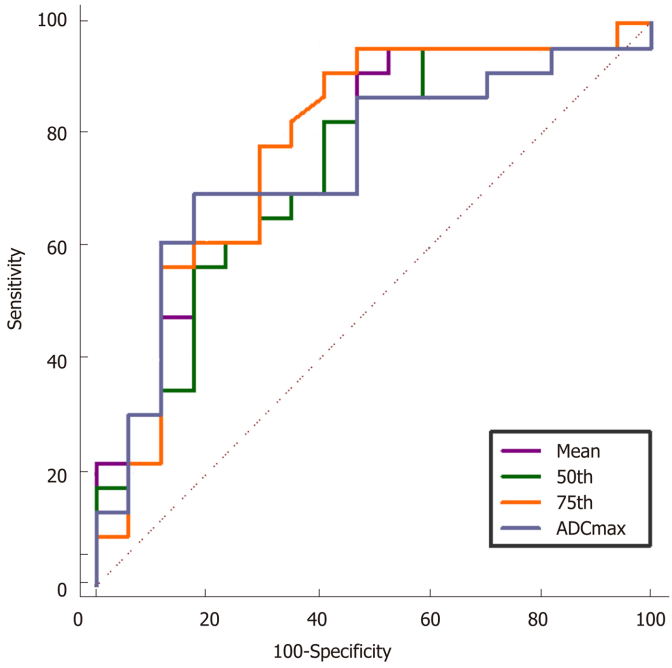

Figure 3 Receiver operating characteristic curves for the volumetric histogram parameters in differentiating intestinal-type periampullary adenocarcinoma from pancreatobiliary-type periampullary adenocarcinoma. ADC: Apparent diffusion coefficient.

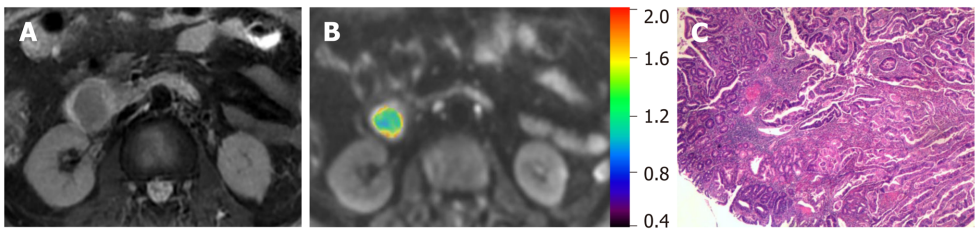

Figure 4 A 61-year-old man with intestinal-type periampullary adenocarcinoma. A: T2-weighted image; B: Corresponding diffusion-weighted image reconstruction of apparent diffusion coefficient (ADC) values (*b*-value = 1000 s/mm^2, ADC values are given in units of ×10^{-3} mm^2/s); C: Haematoxylin and eosin staining of the lesion (original magnification, ×40).

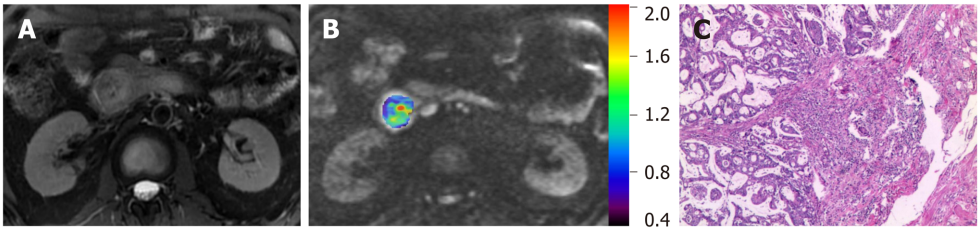

Figure 5 A 49-year-old man with pancreatobiliary-type periampullary adenocarcinoma. A: T2-weighted image; B: Corresponding diffusion-weighted image reconstruction of apparent diffusion coefficient (ADC) values (*b*-value = 1000 s/mm^2, ADC values are given in units of ×10^{-3} mm^2/s); C: Haematoxylin and eosin staining of the lesion (original magnification, ×40).

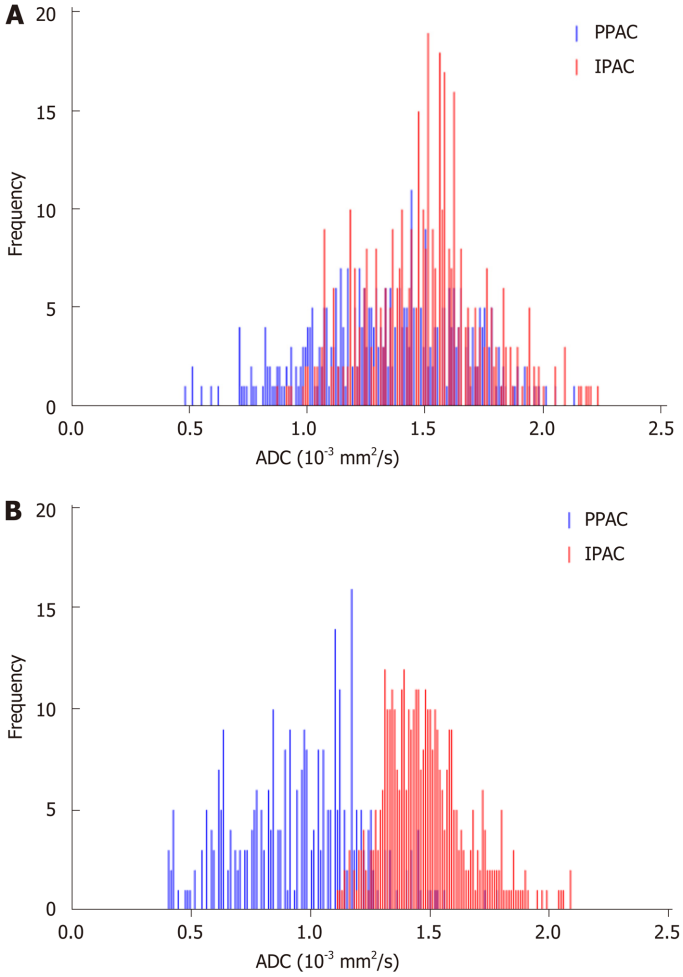

Figure 6 Corresponding volumetric histograms of intestinal-type periampullary adenocarcinoma and pancreatobiliary-type periampullary adenocarcinoma. A: Corresponding volumetric histogram (b_{800}) shows the overlap distribution of ADC values of IPAC and PPAC. For the PPAC, the mean, 50th percentile, 75th percentile, and ADC_{max} were 1.35, 1.38, 1.55, and 2.14 × 10^{-3} mm^2/s, respectively. For the IPAC, the mean, 50th percentile, 75th percentile, and ADC_{max} were 1.52, 1.53, 1.63, and 2.26 × 10^{-3} mm^2/s, respectively; B: Corresponding volumetric histogram (b*1000*) shows a higher ADC distribution range in the IPAC. For the PPAC, the mean, 50th percentile, 75th percentile, and ADC_{max} were 0.96, 0.98, 1.14, and 1.80 ×10^{-3} mm^2/s, respectively. For the IPAC, the mean, 50th percentile, 75th percentile, and ADC_{max} were 1.49, 1.47, 1.58, and 2.10 ×10^{-3} mm^2/s, respectively. IPAC: Intestinal-type periampullary adenocarcinoma; PPAC: Pancreatobiliary-type periampullary adenocarcinoma; ADC: Apparent diffusion coefficient.

ARTICLE HIGHLIGHTS

Research background

The histological heterogeneity of periampullary adenocarcinoma is high as it comprises adenocarcinomas of the ampulla, distal common bile duct, pancreas, and duodenum. Misclassification of the original tumor site occurs in clinical practice, which causes inappropriate postoperative treatment and incorrect prediction of the overall survival. Recently, the histopathological subtype of periampullary adenocarcinomas is demonstrated to be a better

prognostic predictor than the site of origin. According to the endoscopic morphological characteristics of tumor tissue, periampullary adenocarcinoma can be classified into two histological subtypes. One is intestinal-type periampullary adenocarcinoma (IPAC) and the other is pancreatobiliary-type periampullary adenocarcinoma (PPAC). IPAC is reported to have a better prognosis than PPAC.

Research motivation

The classification of histological subtypes is difficult to determine before surgery. Limitations still exist for contrast-enhanced computed tomography or multiparameter magnetic resonance imaging to help differentiating between IPAC and PPAC. Diffusion-weighted imaging (DWI) is a noninvasive functional imaging method. It calculates the apparent diffusion coefficient (ADC) to reflect random motion of water molecules, which could add information pertinent to tissue structure. Based on DWI, ADC histogram analysis has been used in the diagnosis of diseases of many other abdominal organs and is demonstrated to have high reproducibility. It may have the ability to differentiate IPAC from PPAC.

Research objectives

The aim of this study was to investigate the diagnostic value of ADC volumetric histogram analysis in differentiation of IPAC and PPAC. Accurate preoperative differentiation between IPAC and PPAC can help predict the prognosis and make treatment strategy for patients with periampullary adenocarcinoma.

Research methods

Patients who were confirmed with a periampullary adenocarcinoma and underwent MRI at 3.0 T with diffusion-weighted images (*b*-values = 800 and 1000 s/mm^2) before surgery were analyzed. The mean, 5th, 10th, 25th, 50th, 75th, 90th, and 95th percentiles of ADC values and ADC_{min}, ADC_{max}, kurtosis, skewness, and entropy were then obtained from the volumetric histogram analysis. Comparisons were made with an independent Student's *t*-test or Mann-Whitney *U* test. Multiple-class receiver operating characteristic curve analysis was performed to determine and compare the diagnostic value of each significant parameter.

Research results

The mean, maximum, and various percentiles ADC values derived from b_{1000} were lower in the PPAC group than in the IPAC group with statistical significance. The 75th percentile of ADC values achieved the highest area under the curve (AUC) (AUC = 0.781; sensitivity, 91%; specificity, 59%; cut-off value, 1.50 ×10^{-3} mm^2/s).

Research conclusions

Our study showed that volumetric ADC histogram analysis could help classify histopathological subtypes of periampullary adenocarcinoma. In addition, a *b*-value of 1000 s/mm^2 has higher diagnostic value than *b*-value of 800 s/mm^2. The 75th percentile ADC_{1000} value achieved the best diagnostic performance.

Research perspectives

Although volumetric ADC histogram analysis has been demonstrated to have the ability to distinguish between IPAC and PPAC, the optimal *b*-value is still not confirmed. Besides, multiple *b*-value DWI studies may provide more differential diagnostic value. Thus, further investigations are needed.

REFERENCES

1 **Kim JH**, Kim MJ, Chung JJ, Lee WJ, Yoo HS, Lee JT. Differential diagnosis of periampullary carcinomas at MR imaging. *Radiographics* 2002; **22**: 1335-1352 [PMID: 12432106 DOI: 10.1148/rg.226025060]

2 **Soer E**, Brosens L, van de Vijver M, Dijk F, van Velthuysen ML, Farina-Sarasqueta A, Morreau H, Offerhaus J, Koens L, Verheij J. Dilemmas for the pathologist in the oncologic assessment of pancreatoduodenectomy specimens : An overview of different grossing approaches and the relevance of the histopathological characteristics in the oncologic assessment of pancreatoduodenectomy specimens. *Virchows Arch* 2018; **472**: 533-543 [PMID: 29589102 DOI: 10.1007/s00428-018-2321-5]

3 **Westgaard A**, Pomianowska E, Clausen OP, Gladhaug IP. Intestinal-type and pancreatobiliary-type adenocarcinomas: how does ampullary carcinoma differ from other periampullary malignancies? *Ann Surg Oncol* 2013; **20**: 430-439 [PMID: 22956064 DOI: 10.1245/s10434-012-2603-0]

4 **Radojkovic M**, Stojanovic M, Radojković D, Jeremic L, Mihailovic D, Ilic I. Histopathologic differentiation as a prognostic factor in patients with carcinoma of the hepatopancreatic ampulla of Vater. *J Int Med Res* 2018; **46**: 4634-4639 [PMID: 30027790 DOI: 10.1177/0300060518786920]

5 **Kim SM**, Eads JR. Adjuvant and Neoadjuvant Therapy for Resectable Pancreatic and Periampullary Cancer. *Surg Clin North Am* 2016; **96**: 1287-1300 [PMID: 27865278 DOI: 10.1016/j.suc.2016.07.004]

6 **Hester CA**, Dogeas E, Augustine MM, Mansour JC, Polanco PM, Porembka MR, Wang SC, Zeh HJ, Yopp AC. Incidence and comparative outcomes of periampullary cancer: A population-based analysis demonstrating improved outcomes and increased use of adjuvant therapy from 2004 to 2012. *J Surg Oncol* 2019; **119**: 303-317 [PMID: 30561818 DOI: 10.1002/jso.25336]

7 **Williams JL**, Chan CK, Toste PA, Elliott IA, Vasquez CR, Sunjaya DB, Swanson EA, Koo J, Hines OJ, Reber HA, Dawson DW, Donahue TR. Association of Histopathologic Phenotype of Periampullary Adenocarcinomas With Survival. *JAMA Surg* 2017; **152**: 82-88 [PMID: 27732711 DOI: 10.1001/jamasurg.2016.3466]

8 **Bronsert P**, Kohler I, Werner M, Makowiec F, Kuesters S, Hoeppner J, Hopt UT, Keck T, Bausch D,

Wellner UF. Intestinal-type of differentiation predicts favourable overall survival: confirmatory clinicopathological analysis of 198 periampullary adenocarcinomas of pancreatic, biliary, ampullary and duodenal origin. *BMC Cancer* 2013; **13**: 428 [PMID: 24053229 DOI: 10.1186/1471-2407-13-428]

9 **Westgaard A**, Tafjord S, Farstad IN, Cvancarova M, Eide TJ, Mathisen O, Clausen OP, Gladhaug IP. Pancreatobiliary versus intestinal histologic type of differentiation is an independent prognostic factor in resected periampullary adenocarcinoma. *BMC Cancer* 2008; **8**: 170 [PMID: 18547417 DOI: 10.1186/1471-2407-8-170]

10 **Acharya A**, Markar SR, Sodergren MH, Malietzis G, Darzi A, Athanasiou T, Khan AZ. Meta-analysis of adjuvant therapy following curative surgery for periampullary adenocarcinoma. *Br J Surg* 2017; **104**: 814-822 [PMID: 28518410 DOI: 10.1002/bjs.10563]

11 **Chandrasegaram MD**, Chen JW, Price TJ, Zalcberg J, Sjoquist K, Merrett ND. Advances in Molecular Pathology and Treatment of Periampullary Cancers. *Pancreas* 2016; **45**: 32-39 [PMID: 26348463 DOI: 10.1097/MPA.0000000000000385]

12 **Kamarajah SK**. Pancreaticoduodenectomy for periampullary tumours: a review article based on Surveillance, End Results and Epidemiology (SEER) database. *Clin Transl Oncol* 2018; **20**: 1153-1160 [PMID: 29335829 DOI: 10.1007/s12094-018-1832-5]

13 **He C**, Mao Y, Wang J, Duan F, Lin X, Li S. Nomograms predict long-term survival for patients with periampullary adenocarcinoma after pancreatoduodenectomy. *BMC Cancer* 2018; **18**: 327 [PMID: 29580215 DOI: 10.1186/s12885-018-4240-x]

14 **Al-Hawary MM**, Kaza RK, Francis IR. Optimal Imaging Modalities for the Diagnosis and Staging of Periampullary Masses. *Surg Oncol Clin N Am* 2016; **25**: 239-253 [PMID: 27013362 DOI: 10.1016/j.soc.2015.12.001]

15 **Ivanovic AM**, Alessandrino F, Maksimovic R, Micev M, Ostojic S, Gore RM, Mortele KJ. Pathologic Subtypes of Ampullary Adenocarcinoma: Value of Ampullary MDCT for Noninvasive Preoperative Differentiation. *AJR Am J Roentgenol* 2017; **208**: W71-W78 [PMID: 28095024 DOI: 10.2214/AJR.16.16723]

16 **Bi L**, Dong Y, Jing C, Wu Q, Xiu J, Cai S, Huang Z, Zhang J, Han X, Liu Q, Lv S. Differentiation of pancreatobiliary-type from intestinal-type periampullary carcinomas using 3.0T MRI. *J Magn Reson Imaging* 2016; **43**: 877-886 [PMID: 26395453 DOI: 10.1002/jmri.25054]

17 **Chung YE**, Kim MJ, Park MS, Choi JY, Kim H, Kim SK, Lee M, Kim HJ, Choi JS, Song SY, Kim KW. Differential features of pancreatobiliary- and intestinal-type ampullary carcinomas at MR imaging. *Radiology* 2010; **257**: 384-393 [PMID: 20829529 DOI: 10.1148/radiol.10100200]

18 **Pasquini L**, Napolitano A, Visconti E, Longo D, Romano A, Tomà P, Rossi Espagnet MC. Gadolinium-Based Contrast Agent-Related Toxicities. *CNS Drugs* 2018; **32**: 229-240 [PMID: 29508245 DOI: 10.1007/s40263-018-0500-1]

19 **Ramalho J**, Ramalho M. Gadolinium Deposition and Chronic Toxicity. *Magn Reson Imaging Clin N Am* 2017; **25**: 765-778 [PMID: 28964466 DOI: 10.1016/j.mric.2017.06.007]

20 **Li A**, Xing W, Li H, Hu Y, Hu D, Li Z, Kamel IR. Subtype Differentiation of Small (≤ 4 cm) Solid Renal Mass Using Volumetric Histogram Analysis of DWI at 3-T MRI. *AJR Am J Roentgenol* 2018; **211**: 614-623 [PMID: 29812980 DOI: 10.2214/AJR.17.19278]

21 **Donati OF**, Mazaheri Y, Afaq A, Vargas HA, Zheng J, Moskowitz CS, Hricak H, Akin O. Prostate cancer aggressiveness: assessment with whole-lesion histogram analysis of the apparent diffusion coefficient. *Radiology* 2014; **271**: 143-152 [PMID: 24475824 DOI: 10.1148/radiol.13130973]

22 **Paschall AK**, Mirmomen SM, Symons R, Pourmorteza A, Gautam R, Sahai A, Dwyer AJ, Merino MJ, Metwalli AR, Linehan WM, Malayeri AA. Differentiating papillary type I RCC from clear cell RCC and oncocytoma: application of whole-lesion volumetric ADC measurement. *Abdom Radiol* 2018; **43**: 2424-2430 [PMID: 29520425 DOI: 10.1007/s00261-017-1453-4]

23 **Wang F**, Wang Y, Zhou Y, Liu C, Xie L, Zhou Z, Liang D, Shen Y, Yao Z, Liu J. Comparison between types I and II epithelial ovarian cancer using histogram analysis of monoexponential, biexponential, and stretched-exponential diffusion models. *J Magn Reson Imaging* 2017; **46**: 1797-1809 [PMID: 28379611 DOI: 10.1002/jmri.25722]

24 **Xie T**, Zhao Q, Fu C, Bai Q, Zhou X, Li L, Grimm R, Liu L, Gu Y, Peng W. Differentiation of triple-negative breast cancer from other subtypes through whole-tumor histogram analysis on multiparametric MR imaging. *Eur Radiol* 2019; **29**: 2535-2544 [PMID: 30402704 DOI: 10.1007/s00330-018-5804-5]

25 **Kimura W**, Futakawa N, Yamagata S, Wada Y, Kuroda A, Muto T, Esaki Y. Different clinicopathologic findings in two histologic types of carcinoma of papilla of Vater. *Jpn J Cancer Res* 1994; **85**: 161-166 [PMID: 7511574 DOI: 10.1111/j.1349-7006.1994.tb02077.x]

26 **Albores-Saavedra J**, Hruban R, Klimstra D, Zamboni G, Bosman FT CF, Hruban RH, Theise ND. Invasive adenocarcinoma of the ampullary region. Bosman FT CF, Hruban RH, Theise ND. WHO classification of tumours of the digestive system. Lyon, France: IARC, 2010: 87-91

27 **Adsay V**, Ohike N, Tajiri T, Kim GE, Krasinskas A, Balci S, Bagci P, Basturk O, Bandyopadhyay S, Jang KT, Kooby DA, Maithel SK, Sarmiento J, Staley CA, Gonzalez RS, Kong SY, Goodman M. Ampullary region carcinomas: definition and site specific classification with delineation of four clinicopathologically and prognostically distinct subsets in an analysis of 249 cases. *Am J Surg Pathol* 2012; **36**: 1592-1608 [PMID: 23026934 DOI: 10.1097/PAS.0b013e31826399d8]

28 **Zhou H**, Schaefer N, Wolff M, Fischer HP. Carcinoma of the ampulla of Vater: comparative histologic/immunohistochemical classification and follow-up. *Am J Surg Pathol* 2004; **28**: 875-882 [PMID: 15223956 DOI: 10.1097/00000478-200407000-00005]

29 **Kumari N**, Prabha K, Singh RK, Baitha DK, Krishnani N. Intestinal and pancreatobiliary differentiation in periampullary carcinoma: the role of immunohistochemistry. *Hum Pathol* 2013; **44**: 2213-2219 [PMID: 23834763 DOI: 10.1016/j.humpath.2013.05.003]

30 **Sandhu V**, Bowitz Lothe IM, Labori KJ, Lingjærde OC, Buanes T, Dalsgaard AM, Skrede ML, Hamfjord J, Haaland T, Eide TJ, Børresen-Dale AL, Ikdahl T, Kure EH. Molecular signatures of mRNAs and miRNAs as prognostic biomarkers in pancreatobiliary and intestinal types of periampullary adenocarcinomas. *Mol Oncol* 2015; **9**: 758-771 [PMID: 25579086 DOI: 10.1016/j.molonc.2014.12.002]

31 **Kalluri Sai Shiva UM**, Kuruva MM, Mitnala S, Rupjyoti T, Guduru Venkat R, Botlagunta S, Kandagaddala R, Siddapuram SP, Sekaran A, Chemalakonda R, Rebala P, Duvvuru NR. MicroRNA profiling in periampullary carcinoma. *Pancreatology* 2014; **14**: 36-47 [PMID: 24555977 DOI: 10.1016/j.pan.2013.10.003]

32 **Sandhu V**, Wedge DC, Bowitz Lothe IM, Labori KJ, Dentro SC, Buanes T, Skrede ML, Dalsgaard AM, Munthe E, Myklebost O, Lingjærde OC, Børresen-Dale AL, Ikdahl T, Van Loo P, Nord S, Kure EH. The

Genomic Landscape of Pancreatic and Periampullary Adenocarcinoma. *Cancer Res* 2016; **76**: 5092-5102 [PMID: 27488532 DOI: 10.1158/0008-5472.CAN-16-0658]

33 **Surov A**, Meyer HJ, Wienke A. Correlation between apparent diffusion coefficient (ADC) and cellularity is different in several tumors: a meta-analysis. *Oncotarget* 2017; **8**: 59492-59499 [PMID: 28938652 DOI: 10.18632/oncotarget.17752]

34 **Koh DM**, Collins DJ. Diffusion-weighted MRI in the body: applications and challenges in oncology. *AJR Am J Roentgenol* 2007; **188**: 1622-1635 [PMID: 17515386 DOI: 10.2214/AJR.06.1403]

35 **Meyer HJ**, Leifels L, Hamerla G, Höhn AK, Surov A. ADC-histogram analysis in head and neck squamous cell carcinoma. Associations with different histopathological features including expression of EGFR, VEGF, HIF-1α, Her 2 and p53. A preliminary study. *Magn Reson Imaging* 2018; **54**: 214-217 [PMID: 30189236 DOI: 10.1016/j.mri.2018.07.013]

36 **Iima M**, Le Bihan D. Clinical Intravoxel Incoherent Motion and Diffusion MR Imaging: Past, Present, and Future. *Radiology* 2016; **278**: 13-32 [PMID: 26690990 DOI: 10.1148/radiol.2015150244]

37 **Padhani AR**, Liu G, Koh DM, Chenevert TL, Thoeny HC, Takahara T, Dzik-Jurasz A, Ross BD, Van Cauteren M, Collins D, Hammoud DA, Rustin GJ, Taouli B, Choyke PL. Diffusion-weighted magnetic resonance imaging as a cancer biomarker: consensus and recommendations. *Neoplasia* 2009; **11**: 102-125 [PMID: 19186405 DOI: 10.1593/neo.81328]

38 **Liu Y**, Zhang Y, Cheng R, Liu S, Qu F, Yin X, Wang Q, Xiao B, Ye Z. Radiomics analysis of apparent diffusion coefficient in cervical cancer: A preliminary study on histological grade evaluation. *J Magn Reson Imaging* 2019; **49**: 280-290 [PMID: 29761595 DOI: 10.1002/jmri.26192]

39 **Chen L**, Shen F, Li Z, Lu H, Chen Y, Wang Z, Lu J. Diffusion-weighted imaging of rectal cancer on repeatability and cancer characterization: an effect of b-value distribution study. *Cancer Imaging* 2018; **18**: 43 [PMID: 30442202 DOI: 10.1186/s40644-018-0177-1]

40 **Guo Y**, Kong QC, Zhu YQ, Liu ZZ, Peng LR, Tang WJ, Yang RM, Xie JJ, Liu CL. Whole-lesion histogram analysis of the apparent diffusion coefficient: Evaluation of the correlation with subtypes of mucinous breast carcinoma. *J Magn Reson Imaging* 2018; **47**: 391-400 [PMID: 28640538 DOI: 10.1002/jmri.25794]

41 **Onodera K**, Hatakenaka M, Yama N, Onodera M, Saito T, Kwee TC, Takahara T. Repeatability analysis of ADC histogram metrics of the uterus. *Acta Radiol* 2019; **60**: 526-534 [PMID: 29969050 DOI: 10.1177/0284185118786062]

42 **Just N**. Improving tumour heterogeneity MRI assessment with histograms. *Br J Cancer* 2014; **111**: 2205-2213 [PMID: 25268373 DOI: 10.1038/bjc.2014.512]

43 **Umanodan T**, Fukukura Y, Kumagae Y, Shindo T, Nakajo M, Takumi K, Nakajo M, Hakamada H, Umanodan A, Yoshiura T. ADC histogram analysis for adrenal tumor histogram analysis of apparent diffusion coefficient in differentiating adrenal adenoma from pheochromocytoma. *J Magn Reson Imaging* 2017; **45**: 1195-1203 [PMID: 27571307 DOI: 10.1002/jmri.25452]

44 **Zou X**, Luo Y, Li Z, Hu Y, Li H, Tang H, Shen Y, Hu D, Kamel IR. Volumetric Apparent Diffusion Coefficient Histogram Analysis in Differentiating Intrahepatic Mass-Forming Cholangiocarcinoma from Hepatocellular Carcinoma. *J Magn Reson Imaging* 2019; **49**: 975-983 [PMID: 30277628 DOI: 10.1002/jmri.26253]

Published By Baishideng Publishing Group Inc
7041 Koll Center Parkway, Suite 160, Pleasanton, CA 94566, USA
Telephone: +1-925-2238242
E-mail: bpgoffice@wjgnet.com
Help Desk:http://www.f6publishing.com/helpdesk
http://www.wjgnet.com